

# Output coupling and flow of a dilute Bose-Einstein condensate

B. Jackson, J. F. McCann, and C. S. Adams

*Dept. of Physics, Rochester Building, University of Durham, South Road, Durham, DH1 3LE, UK.*

(June 17, 2018)

We solve the Gross-Pitaevskii equation to model the behaviour of a weakly-interacting Bose condensate. Solutions are presented for the eigenstates in one- and two-dimensional harmonic traps. We include the effect of gravity and coupling to a second condensate to simulate an output coupler for Bose condensed atoms, and find that the output pulse shape is in qualitative agreement with experiment. We also model flow under gravity through a constriction, demonstrating excitation and separation of eigenmodes in the condensate.

## I. INTRODUCTION

The first experimental observations of Bose-Einstein condensation in magnetically-trapped alkali atoms [1–3] excited considerable interest in the properties of weakly-interacting Bose fluids. Subsequent experiments have studied collective excitations [4,5] and sound propagation in the condensate [6,7], leading to hopes of a deeper understanding of the nature of superfluidity [8]. An important recent experiment has shown macroscopic interference between two expanding condensates, providing compelling evidence for coherence in the ground state of the trap [9]. Thus, the demonstration of an output coupler for Bose condensed atoms [10] may be thought of as realizing a simple pulsed atom laser, though controversy still surrounds this issue [11].

Theoretical work on weakly-interacting Bose condensates has focused on solutions of the Gross-Pitaevskii or time-dependent nonlinear Schrödinger equation (NLSE) [12–15]. This equation describes the evolution of a self-consistent wavefunction representing a dilute near-zero temperature condensate, and follows from mean-field theory where interactions between atoms are modelled by an  $s$ -wave scattering length [16]. The Gross-Pitaevskii equation has been shown to provide an accurate description of the shape [15] and dynamics [4,5,17] of weakly interacting condensates, with the principal effect of finite temperature arising as condensate depletion [18].

The time-dependent NLSE may be solved numerically by a variety of methods [19]. Previous studies have used semi-implicit Crank-Nicholson in one dimension [13], or alternating-direction implicit-difference in two dimensions [15]. In this work, we solve the NLSE using Split-Step Fourier [19,20] and finite difference methods. A combination of these techniques can be used to model the dynamics of a condensate under a wide range of situations, for example, the creation of vortices by a moving object [21].

Here we consider two examples: simulations of the output coupling of Bose condensed atoms from a trap; and the flow of a condensate through a constriction. The output coupling of Bose condensed atoms, by driving an RF transition to a untrapped state, has been demonstrated experimentally by Mewes *et al.* [10]. Previous theoretical studies have considered only 1D motion without gravity [22], or have modelled the process by neglecting kinetic energy [23] or interaction terms [24] in the Gross-Pitaevskii equation. We solve coupled Gross-Pitaevskii equations in 2D, with the inclusion of gravity, to model the evolution of both the output pulse and the remaining trapped condensate. The simulations reproduce the crescent-shaped atomic pulses observed experimentally [10,25], and we demonstrate that the recoil of the output pulse excites a harmonic oscillation of the parent condensate. Secondly, we consider techniques for condensate manipulation. To maintain the shape of a condensate pulse, it could be coupled into a waveguide such as a collimated far-off resonance laser beam. However, a more interesting situation arises in the flow through a constriction. For this case, we predict the excitation and spatial filtering of eigenmodes.

The paper is arranged as follows: Section 2 contrasts the Fourier and finite-difference methods, and discusses 1D and 2D solutions of the Gross-Pitaevskii equation for the lowest energy levels. Simulations of the output coupling and flow through a constriction are presented in Sections 3 and 4 respectively.

## II. NUMERICAL SOLUTION OF THE GROSS-PITAIEVSKII EQUATION

The property of phase coherence inherent in Bose condensation implies that it may be represented by an order parameter, which is simply the macroscopic wavefunction of the condensate. At zero temperature this wavefunction,  $\Psi(\mathbf{r}, t)$ , is described by the Gross-Pitaevskii equation. Including a trap potential,  $V(\mathbf{r}, t)$ , this has the form [26]:

$$i\hbar \frac{\partial}{\partial t} \Psi(\mathbf{r}, t) = \left( -\frac{\hbar^2}{2m} \nabla^2 + V(\mathbf{r}, t) + NU_0 |\Psi(\mathbf{r}, t)|^2 \right) \Psi(\mathbf{r}, t), \quad (1)$$

where  $m$  is the atomic mass,  $N$  is the number of atoms, and  $U_0$  describes the interaction between atoms in the condensate. For  $T \approx 0$  interactions are modelled by the  $s$ -wave scattering length,  $a$ , such that  $U_0 = 4\pi\hbar^2 a/m$ .

First, consider a 1D condensate, where the trapping potential is described by  $V(x) = m\omega^2 x^2/2$ . For convenience, equation (1) is scaled in terms of harmonic oscillator units (h.o.u.) of length and time, where  $\xi = (\hbar/2m\omega)^{-1/2} x$  and  $\tau = \omega t$ . With the change in length scale the normalisation of the wavefunction is also modified, and thus  $\psi(\xi, \tau) = (\hbar/2m\omega)^{1/4} \Psi(x, t)$ . Taking the unit of energy to be  $\hbar\omega$ , equation (1) becomes [13]:

$$i \frac{\partial}{\partial \tau} \psi(\xi, \tau) = \left( -\frac{\partial^2}{\partial \xi^2} + \frac{1}{4} \xi^2 + C |\psi(\xi, \tau)|^2 \right) \psi(\xi, \tau), \quad (2)$$

where  $C = 4\pi Na(2\hbar/m\omega)^{1/2}$ . In the next two subsections, we discuss the solution of this NLSE using (A) the Split-Step Fourier method, and (B) finite differences.

### A. Fourier method

Consider a Schrödinger equation of the form:

$$i\hbar \frac{\partial}{\partial t} \psi(\mathbf{r}, t) = [T + V(\mathbf{r}, t)] \psi(\mathbf{r}, t) = H(\mathbf{r}, t) \psi(\mathbf{r}, t), \quad (3)$$

with the solution,  $\psi(\mathbf{r}, 0)$ , at  $t = 0$ . We can propagate the solution through a short time interval to second-order accuracy using the unitary evolution operator. Expansion of the time-evolution operator gives [28]:

$$e^{-iHt/\hbar} \approx e^{-iV(0)t/2\hbar} e^{-iTt/\hbar} e^{-iV(0)t/2\hbar} + O(t^2). \quad (4)$$

For a slowly-varying  $V(t)$ , the order of accuracy of this ‘half-step’ expansion increases to  $O(t^3)$ . The operator,  $\exp(-iTt/\hbar)$  can be evaluated numerically by a variety of methods [19]. The Split-Step Fourier method relies on the use of discrete Fourier transforms computed with a Fast Fourier Transform (FFT) algorithm, allowing high computational efficiency. Moreover, the Split-Step Fourier method is readily extended to solution of the NLSE in an arbitrary number of dimensions by use of  $N$ -dimensional FFT routines [27].

Solutions of (2) may be evaluated numerically by beginning with an analytic ground or excited state solution in the absence of the nonlinear term. The solution is then propagated through real time using the Split-Step Fourier method, while at each time step, the value of the nonlinear constant  $C$  is increased adiabatically (‘ramped’) until reaching the desired value of  $C$ . In practice, this consists of inserting a time-dependent pre-factor,  $P(\tau) = [1 - \cos(\pi\tau/\tau_r)]/2$ , in front of the nonlinear term [15], where the ramp time  $\tau_r$  is chosen to be long compared to the oscillation time of the ground state of the trap. Alternatively, the ground state can be readily determined through propagation in imaginary time ( $t \rightarrow -i\tilde{t}$ ) [20]. However, we find that imaginary time FFT is inappropriate for the excited states, as these are exponentially suppressed with respect to lower energy modes.

One-dimensional wavefunctions for the first and second excited states are presented in Figs. 1 and 2, and show interesting behaviour as the repulsive interactions increase in strength. In both cases, the edges of

the wavefunction spread out in a similar fashion to the ground state [13]. However, for the first excited state the width of the central node barely changes as  $C$  increases; while in the second excited state, the two nodes of the symmetric condensate asymptotically approach a fixed separation,  $\Delta\xi \sim 1$ , for large  $C$ . Later, we will demonstrate how such modes could be excited by flow of a condensate through a constriction (Section 4).

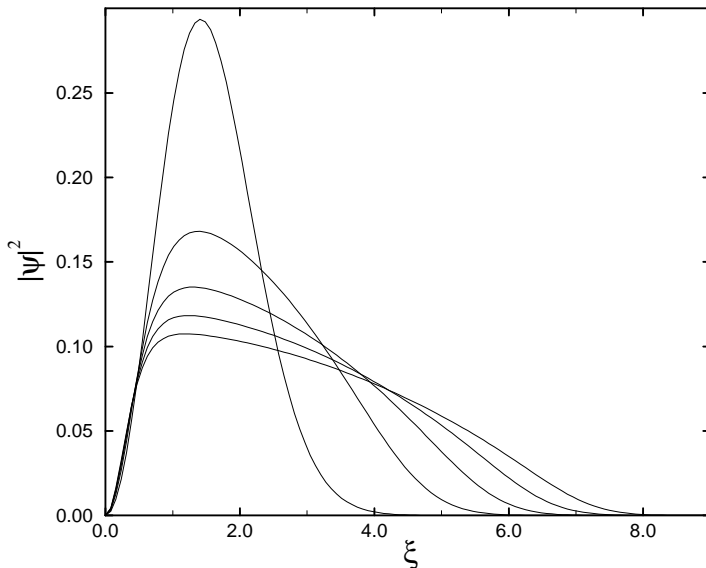


FIG. 1. Condensate density  $|\psi|^2$  plotted against position (in h.o.u.) for the first excited state in 1D, with the nonlinear coefficient  $C = 0, 30, 60, 90, 120$ . As  $C$  increases, the edges of the symmetric condensate spread out while the central node remains almost unchanged.

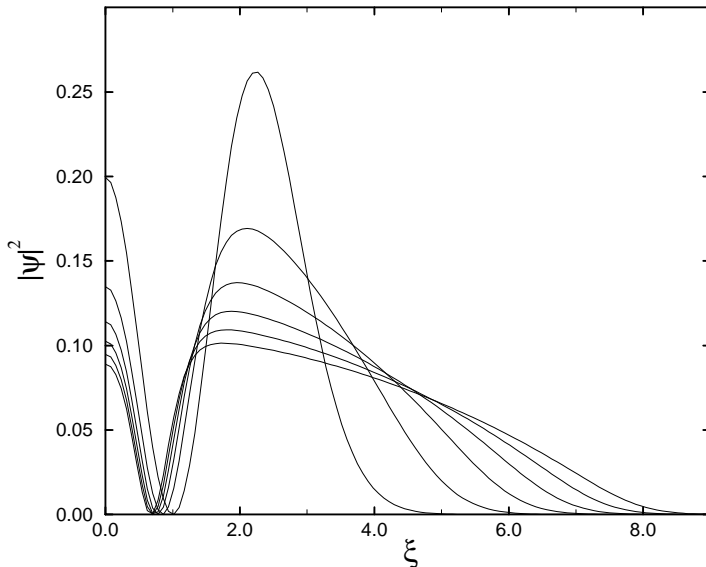


FIG. 2. Condensate density  $|\psi|^2$  plotted against position (in h.o.u.) for the second excited state in 1D, for  $C = 0, 30, 60, 90, 120, 150$ . As the interactions increase the nodes of the symmetric condensate converge, and tend towards a fixed separation at high  $C$ .

## B. Finite differences

The procedure described above is difficult to implement for  $C > 150$ , requiring long computation times—a problem compounded in 2D. An alternative approach is to evaluate the solutions of the NLSE and corresponding chemical potentials using finite differences. By replacing the differentials in (2) by finite differences between all adjacent grid points, and including the condition that the wavefunction is normalised, we obtain a set of simultaneous equations for values of the wavefunction at each grid point. The simultaneous nonlinear equations can then be solved by iteration, e.g. using the Newton-Raphson method. Table I displays chemical potentials for the ground and first two excited states of the trap, in units of  $\hbar\omega$ . By neglecting the kinetic term in the time-independent NLSE—an approximation valid for large interaction strengths—one obtains a simple analytic solution for the ground state [12], for which the chemical potential is  $\mu_{1D} = (3C/8)^{2/3}$ . This is commonly known as the Thomas-Fermi approximation. At large  $C$ , the data for the ground state does indeed approach the Thomas-Fermi limit. In addition, the ground and excited energies converge so that they approach a fixed, equal separation at high  $C$ . For a 2D isotropic trap,  $V(x, z) = m\omega^2(x^2 + z^2)/2$ , we can reduce the problem to 1D by converting to cylindrical polar coordinates. Then the eigenvalue equation has the form:

$$\left( -\frac{\partial^2}{\partial \rho^2} - \frac{1}{\rho} \frac{\partial}{\partial \rho} - \frac{1}{\rho^2} \frac{\partial^2}{\partial \varphi^2} + \frac{1}{4} \rho^2 - \mu + C|\psi(\rho, \varphi, \tau)|^2 \right) \psi(\rho, \varphi, \tau) = 0, \quad (5)$$

where the ground state (i.e. no  $\varphi$ -dependence) is to be found. Ground-state chemical potentials for the 2D circular trap are presented in Table I. An important point to note is that the results approach the Thomas-Fermi limit,  $\mu_{2D} = (C/2\pi)^{1/2}$ , more slowly than in 1D. The parabolic Thomas-Fermi wavefunction fails to match the exact solution at the edges of the condensate. In 1D the wavefunctions mismatch at only two points, while in 2D the mismatched region is a ring. Thus, as the dimensionality of the condensate increases, the Thomas-Fermi solution attains less accuracy, and one must be cautious when using this approximation in 3D.

This example also illustrates the ease with which the finite-difference method can find solutions of a NLSE containing large nonlinearities, when compared to the Split-Step Fourier method. However, our experience, in agreement with detailed studies [19], indicates that the Fourier method is more efficient when propagating the solution subject to a time-dependent potential. This is of particular significance when considering 2D simulations, where it is important that the computational times remain manageable. So, in the 2D simulations contained in this paper, we first find the ground-state solution of the NLSE for a trapped condensate using the finite difference method, and then propagate the wavefunction under a time-dependent potential using the Split-Step Fourier method.

TABLE I. Chemical potentials (in units of  $\hbar\omega$ ) for the three lowest energy states in 1D, and for the ground state of an isotropic 2D condensate, calculated using finite differences. Ground state values are compared to the corresponding Thomas-Fermi values:  $\mu_{1D} = (3C/8)^{2/3}$  and  $\mu_{2D} = (C/2\pi)^{1/2}$ .

C	1D				2D	
	Ground state		Excited states		Ground state	
	Numerical solution	Thomas-Fermi	First	Second	Numerical solution	Thomas-Fermi
0	0.500	0.000	1.500	2.500	1.000	0.000
10	2.493	2.414	3.266	4.107	1.620	1.262
20	3.886	3.832	4.630	5.427	2.064	1.784
30	5.065	5.021	5.798	6.576	2.426	2.185
50	7.091	7.058	7.816	8.576	3.020	2.821
100	11.23	11.20	11.94	12.69	4.143	3.989
200	17.80	17.78	18.51	19.24	5.760	5.642
500	32.77	32.76	33.48	34.20	9.003	8.921

### III. THE OUTPUT COUPLER

#### A. The coupled Gross-Pitaevskii equations

The previous section discussed how a combination of Fourier and finite difference methods are particularly efficient at finding and propagating solutions of the Gross-Pitaevskii equation. The same technique can be applied to mixtures of condensates. In particular, we solve coupled equations to describe the experimental realization of an output coupler for Bose condensed atoms, where a sequence of ‘daughter’ condensate pulses is produced by excitation of a ‘parent’ condensate [10]. For  $^{23}\text{Na}$  (or  $^{87}\text{Rb}$  [1]) condensates, the  $F = 1$  ground state is composed of the trapped state  $M_F = -1$ , the magnetically insensitive level  $M_F = 0$ , and the anti-trapped state  $M_F = 1$ . Condensed atoms in each state may be represented by a Bose wavefunction  $\Psi_i(\mathbf{r}, t)$ , where  $i \in \{-1, 0, +1\}$ . The Hamiltonian of the system can then be constructed, to include gravitational and magnetic trapping potentials, hyperfine interactions, and the RF coupling term  $-\boldsymbol{\mu} \cdot \mathbf{B}(\mathbf{r}, t)$ . Our approach involves applying the variational principle to obtain the following equations describing the dynamics of the parent ( $\Psi_{-1}$ ) and daughter condensates ( $\Psi_0, \Psi_1$ ):

$$i\hbar \frac{\partial}{\partial t} \Psi_k(\mathbf{r}, t) = \left[ -\frac{\hbar^2}{2m} \nabla^2 + U_k(\mathbf{r}) + N \sum_j \langle \Psi_j | V | \Psi_j \rangle \right] \Psi_k(\mathbf{r}, t) + \hbar \sum_{j \neq k} \Omega_{kj} \Psi_j(\mathbf{r}, t), \quad (6)$$

where  $U_k(\mathbf{r})$  represents the gravitational and trap potentials in the substate  $k$ , and  $\Omega_{kj}$  is the Rabi frequency describing coupling between sublevels. Atom-atom scattering appears as the matrix element  $\langle \Psi_j | V | \Psi_j \rangle$ . Assuming all scattering lengths to be equal,  $V$  may be replaced by the pseudopotential  $U_0 \delta(\mathbf{r}_i - \mathbf{r}_j)$ .

In the experiment, the RF pulse was of short duration and small area [10], leading to the following simplifications. First, due to the small area ( $|\int \Omega_{+1,0} dt| \ll 1$ ), coupling to the  $M_F = -1$  state is small and may be safely ignored, and also back-coupling, i.e. Rabi oscillations, are negligible. An example of strong coupling, where Rabi oscillations are important, has been considered by Ballagh *et al.* [22] in a 1D weightless model. Secondly, the short pulse duration,  $T$  results in broadband excitation, so that we may assume resonant coupling across the trap and neglect the spatial dependence of the coupling term,  $\Omega(\mathbf{r}, t)$ . In addition, we may assume that the parent condensate is ‘frozen’ during the interaction ( $\omega T \ll 1$ ), in which case the daughter condensate is created suddenly as a shadow of the parent, i.e.:

$$|\Psi_0(\mathbf{r}, T)|^2 \approx \left| -i \int_0^T dt' \Omega(\mathbf{r}, t') \Psi_{-1}(\mathbf{r}, t') \right|^2 \approx f |\Psi_{-1}(\mathbf{r}, 0)|^2, \quad (7)$$

and,

$$|\Psi_{-1}(\mathbf{r}, T)|^2 \approx (1 - f) |\Psi_{-1}(\mathbf{r}, 0)|^2, \quad (8)$$

where  $f$ , the fraction of atoms coupled out of the trap, is equal to the square of the pulse area. Following these simplifications, we obtain a pair of coupled time-dependent equations in 2D:

$$i\partial_\tau \psi_{-1} = (-\nabla^2 + \frac{1}{4}(\xi^2 + \eta^2) + C|\psi_{-1}|^2 + C|\psi_0|^2) \psi_{-1}, \quad (9)$$

$$i\partial_\tau \psi_0 = (-\nabla^2 + G\eta + C|\psi_0|^2 + C|\psi_{-1}|^2) \psi_0, \quad (10)$$

where  $\xi = (\hbar/2m\omega)^{-1/2}x$ ,  $\eta = (\hbar/2m\omega)^{-1/2}z$ , and  $\psi_i(\xi, \eta, \tau) = (\hbar/2m\omega)^{-1/2}\Psi_i(x, z, t)$ . Thus,  $C = 8\pi Na$ , where  $N$  is the linear density of atoms in the  $y$ -direction, and gravity is parametrized by  $G = (m/2\hbar\omega^3)^{1/2}g$ . Note that gravity is absent from Equation (9), as this term only gives rise to displacement of the equilibrium position of the trapped condensate. With initial conditions given by Equations (7) and (8), equations (9) and (10) are solved to model the dynamical behaviour of the parent and daughter condensates for  $\tau \geq \omega T$ . The results of these simulations are now discussed.

## B. Results

To simulate the MIT experiment we consider the parameters  $C = 200$  and  $G = 3.0$ , corresponding to a trap frequency of  $\omega \simeq 2\pi \times 200$  Hz and  $N \approx 2 \times 10^4$   $^{23}\text{Na}$  atoms per h.o.u. respectively. Density plots of the output pulse (for  $f = 0.2$ ) are presented in Fig. 3. After creation, the output pulse is subject to gravity, a repulsive internal force, and a strong repulsion from the residual parent condensate. We see in Fig. 3 that even at early times, a combination of these effects dramatically changes the shape of the output. The curvature of the daughter condensate is found to be less pronounced for weaker interaction strengths. At later times the output pulse expands freely, resulting in a ‘crescent-shaped’ density profile, characteristic of the MIT experiment [10,25]. This suggests that the zero-temperature approximation, inherent in the coupled Gross-Pitaevskii equations, is appropriate for modelling the dynamics of the output. The curvature of the output pulse was not observed in previous theoretical studies [24], due to a different trap geometry and subsequent neglect of the interaction term in the axial direction.

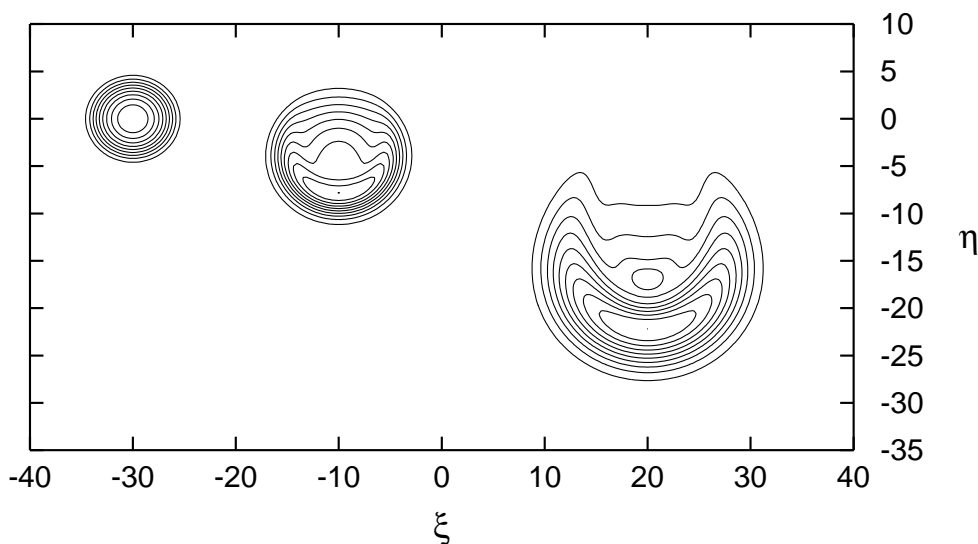


FIG. 3. Contour plot of  $|\psi(\xi, \eta, \tau)|^2$  for an output coupled Bose condensate falling under gravity, with  $C = 200$ ,  $f = 0.20$  and  $G = 3.0$ , at times  $\tau = 0$  (offset  $\xi \rightarrow \xi - 30$ ),  $\tau = 1.2$  (offset  $\xi \rightarrow \xi - 10$ ), and  $\tau = 2.4$  (offset  $\xi \rightarrow \xi + 20$ ). Nine equally-spaced contours are drawn for each time-frame, up to peak densities of  $|\psi(0, 0, 0)|^2 = 5.67 \times 10^{-3}$ ,  $|\psi(0, -7.8125, 1.2)|^2 = 2.36 \times 10^{-3}$ , and  $|\psi(0, -22.1875, 2.4)|^2 = 1.25 \times 10^{-3}$ . The repulsive force from the condensate remaining in the trap, combined with free expansion under gravity, creates a ‘crescent-shaped’ profile in the output.

The mutual repulsion between parent and daughter leads to a small recoil of the more massive, trapped condensate. The subsequent motion of the parent can be inferred by studying its centre of mass, given by  $\eta_c = \int \int \eta |\psi|^2 d\xi d\eta$ . Simulations of a condensate in free-fall show that calculations of the centre of mass agree with the classical result,  $\eta_c = -G\tau^2$ , to five significant figures. The centre of mass coordinate of the parent condensate along with its second time derivative (acceleration), are displayed in Fig. 4. The repulsive force from the output pulse reaches a maximum at  $\tau \sim 0.75$ . Subsequently, as the coupling term falls to zero due to the decreasing overlap, the parent undergoes harmonic motion at the trap frequency, as expected. Fig. 4 also illustrates that the recoil is less for smaller output fractions. Given that the output coupling for small  $f$  does not seriously perturb the parent, further coherent pulses may be produced, and one would expect that the recoil on the parent would be negligible for slow, continuous output coupling. Given the agreement between these dynamical simulations and experiment, we surmise that the same numerical methods can be employed to model the dynamics of the condensate in other interesting situations. An example is discussed in the following section.

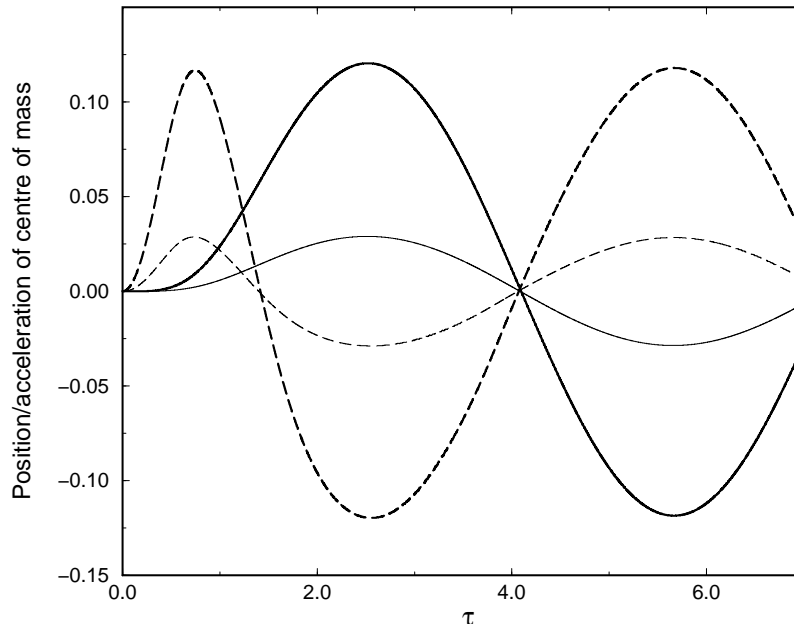


FIG. 4. The vertical position (solid line) and acceleration (dashed) of the centre of mass of the trapped parent condensate ( $C = 200$  and  $G = 3.0$ ) as a function of time. Repulsion from the output pulse induces a recoil, which excites the parent into simple harmonic motion. Results are presented for  $f = 0.20$  (thick lines) and  $f = 0.05$  (thin lines).

#### IV. FLOW THROUGH A CONSTRICTION

We now consider the flow of a weakly-interacting condensate through a constriction. In the 2D simulations presented here, the condensate is released from a circular trap and falls under gravity down a focused, far-off resonance laser beam. The beam is approximated by a harmonic potential in which the spring constant varies with position along  $z$ . Any variation in potential along the  $z$ -axis (e.g. due to an increase in intensity near to the focus) is neglected. This situation may be realized using a blue-detuned doughnut mode laser (see e.g. [29]). The model also assumes that there is no delay between release from the trap and switching on the laser beam. Under this model, for  $\tau > 0$ , the evolution of the condensate is given by the equation:

$$i\partial_\tau\psi = \left( -\nabla^2 + \frac{1}{4} \left[ \frac{1 + (\eta_m^2/\eta_0^2)}{1 + (\eta - \eta_m)^2/\eta_0^2} \right]^2 \xi^2 + G\eta + C|\psi|^2 \right) \psi, \quad (11)$$

so that the horizontal oscillation frequency,  $\omega = (\eta_0^2 + \eta_m^2)/[\eta_0^2 + (\eta - \eta_m)^2]$ , is matched to the initial trap frequency at the ‘release’ position,  $\eta = 0$ , and increases by a factor of  $[1 + (\eta_m/\eta_0)^2]$  at  $\eta = \eta_m$ . The limit  $\eta_0 \rightarrow \infty$  corresponds to a collimated laser beam. In this case, the simulations show that the laser acts as a waveguide for output-coupled condensates.

An interesting situation arises when the laser is tightly-focused. Fig. 5 displays results of the simulation for a small nonlinear coefficient ( $C = 10$ ). The density plot at  $\tau = 2.0$  illustrates that three peaks are formed above the constriction. Scaling the 1D wavefunctions in Section 2 illustrates that the peaks approximately match the positions of the maxima in Fig. 2, suggesting that the second excited state is populated and therefore parity is conserved. The probability that the condensate will be excited from the ground state is related to the rate of change in the Hamiltonian compared to the excitation spectrum. For example, in the non-interacting limit ( $C \rightarrow 0$ ), we can derive an approximate criterion for excitation to occur based on adiabaticity:  $4G^{1/2}|\eta_m|^{1/2}/\eta_0 \gg \Delta\mu$ , where  $\Delta\mu$  is the difference in energy between the ground and excited states. Thus, a small constriction creates a sudden change in the Hamiltonian

and mode excitation occurs. Conversely, for wider constrictions, the Hamiltonian changes slowly and the fluid can adjust adiabatically.

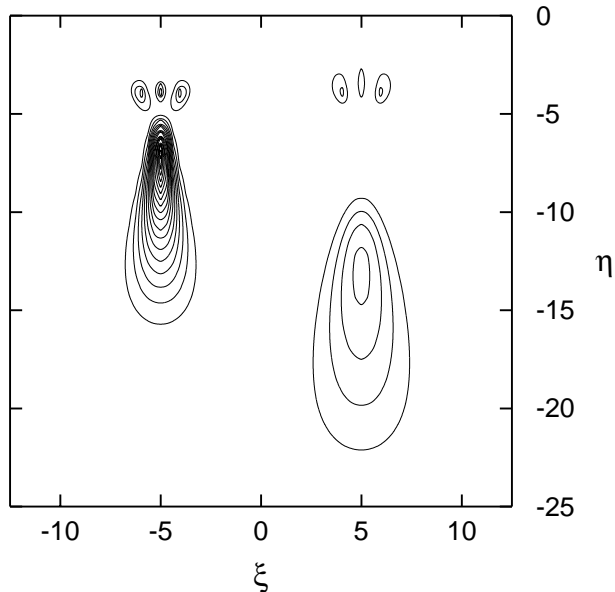


FIG. 5. Flow of a weakly-interacting condensate ( $C = 10$ ,  $G = 3.0$ ) through a constriction, where the oscillation frequency increases by a factor of 11.5 between  $\eta = 0.0$  and  $\eta_m = -6.0$ . Contours of the density are shown at  $\tau = 2.0$  (offset left) and  $\tau = 2.5$  (offset right). The excited ‘tail’ of the condensate remains above the constriction while the ground state falls under gravity, leading to spatial separation of the eigenstates. The contours are drawn with an equal spacing of  $7 \times 10^{-3}$ .

At subsequent times ( $\tau = 2.5$  in Fig. 5) the excited ‘tail’ remains above the constriction, while the ‘bulk’ of the condensate in the ground state continues to fall. To understand this separation of eigenmodes, consider the simple case of a non-interacting condensate,  $C = 0$ . As the condensate falls into the constriction, the increase in oscillation frequency,  $\delta\omega$ , leads to a rise in the chemical potential by  $\delta\mu = (n + 1/2)\delta\omega$ . This increase in energy is provided by a change in the gravitational potential,  $G\eta$ . Equating these energies gives an expression for the equilibrium position,  $\eta_e$ :

$$\eta_e = \eta_m + \frac{(n + \frac{1}{2})}{2G} + \sqrt{\frac{(n + \frac{1}{2})^2}{4G^2} - \frac{\eta_m (n + \frac{1}{2})}{G} - \eta_0^2}, \quad (12)$$

So, for the  $n$ -th mode to be trapped, the following inequality must hold:

$$n \geq 2G \left( \eta_m + \sqrt{\eta_m^2 + \eta_0^2} \right) - \frac{1}{2}. \quad (13)$$

In the case of Fig. 5, equation (12) predicts  $\eta_e \simeq -4.3$  for  $n = 2$ , just below the actual position as expected, because the small nonlinearity tends to push the mode upwards. In addition, the inequality (13) gives  $n > 1.2$ , confirming that only excited states are trapped above the constriction. The constriction thus acts as a mode ‘filter’, and could provide a convenient means to generate and study the decay of excitations. However, for a light-induced potential this would require tight-focusing: typically spot sizes of  $1 \mu\text{m}$  or less.

For large  $C$ , the interaction term in the chemical potential dominates. Thus, in addition to the rise in energy due to the changing  $\omega$ , there is an increase in the density and therefore the interaction energy. As a result, the relative difference between eigenvalues is much lower than for  $C = 0$ , and mode separation tends not to occur. In Fig. 6, one can see that, for  $C = 200$ , two maxima form above a wide constriction. Parity is still conserved, but the ‘tail’ in this case consists mainly of a superposition of ground and second excited states. If narrower constrictions are used, many modes are excited, and the situation becomes increasingly complex.



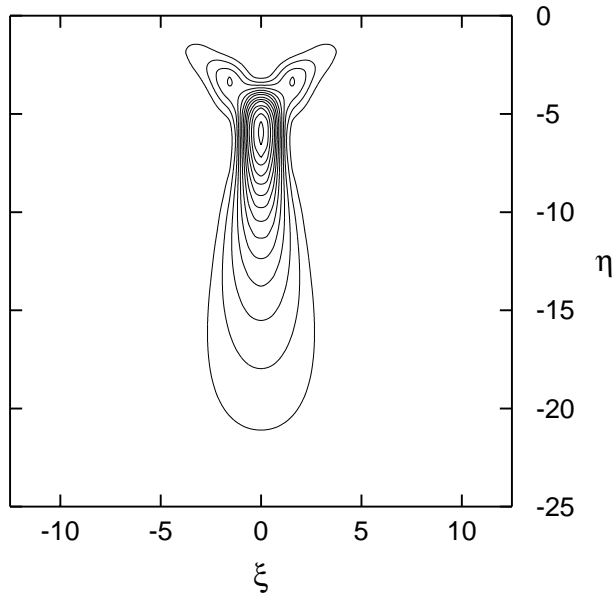


FIG. 6. Flow of a condensate ( $C = 200$ ,  $G = 3.0$ ) through a constriction at a time  $\tau = 2.0$ , where the oscillation frequency increases by a factor of 2.5 between  $\eta = 0.0$  and  $\eta = -6.0$ . As for the weakly-interacting case, the potential induces excitations in the condensate. Contours are drawn with an equal spacing of  $3.03 \times 10^{-3}$ .

## V. SUMMARY

In this paper, we present 1D and 2D solutions of the Gross-Pitaevskii equation. 1D wavefunctions for the first and second excited states are presented for various interaction strengths, and provide useful information for the subsequent interpretation of our 2D simulations. 2D ground state solutions are also calculated for a circular geometry using a finite difference method. We note that convergence towards the interaction dominated Thomas-Fermi limit is slower in two than in one dimension.

The 2D wavefunctions were used as initial conditions in the following 2D simulations. Firstly, an output coupler for magnetically-trapped Bose condensed atoms was simulated by solution of a pair of coupled Gross-Pitaevskii equations, to represent the output pulse and parent condensate. We demonstrate that a combination of atomic interactions and gravity leads to curvature in the output, in qualitative agreement with experiment. The simulations also demonstrate that dipolar centre-of-mass modes are excited in the remaining trapped condensate. The amplitude of the mode is particularly sensitive to the output fraction, and could provide a useful diagnostic in experiments. Secondly, we presented simulations of the flow of a condensate dropped under gravity into a tightly-focused laser beam. We demonstrate that a tight constriction may be used to excite and separate eigenmodes in a weakly-interacting condensate. This could provide a useful technique to study the decay of excited condensate modes.

## ACKNOWLEDGMENTS

Financial support for this work was provided by the Nuffield Foundation and the EPSRC.

- 
- [1] Anderson M H, Ensher J R, Matthews M R, Wieman C E and Cornell E A 1995 *Science* **269** 198
  - [2] Davis K B, Mewes M -O, Andrews M R, van Druten N J, Durfee D S, Kurn D M and Ketterle W 1995 *Phys. Rev. Lett.* **75** 3969

- [3] Bradley C C, Sackett C A and Hulet R G 1997 *Phys. Rev. Lett.* **78** 985
- [4] Jin D S, Ensher J R, Matthews M R, Wieman C E and Cornell E A 1996 *Phys. Rev. Lett.* **77** 420
- [5] Mewes M -O, Andrews M R, van Druten N J, Kurn D M, Durfee D S, Townsend C G and Ketterle W 1996 *Phys. Rev. Lett.* **77** 988
- [6] Andrews M R, Kurn D M, Miesner H -J, Durfee D S, Townsend C G, Inouye S and Ketterle W 1997 *Phys. Rev. Lett.* **79** 553
- [7] Stamper-Kurn D M, Miesner H -J, Inouye S, Andrews M R and Ketterle W preprint cond-mat/9801262
- [8] Stringari S 1996 *Phys. Rev. Lett.* **77** 2360
- [9] Andrews M R, Townsend C G, Miesner H -J, Durfee D S, Kurn D M and Ketterle W 1997 *Science* **275** 637
- [10] Mewes M -O, Andrews M R, Kurn D M, Durfee D S, Townsend C G and Ketterle W 1997 *Phys. Rev. Lett.* **78** 582
- [11] Wiseman H M 1997 *Phys. Rev. A* **56** 2068
- [12] Edwards M and Burnett K 1995 *Phys. Rev. A* **51** 1382
- [13] Ruprecht P A, Holland M J, Burnett K and Edwards M 1995 *Phys. Rev. A* **51** 4704
- [14] Edwards M, Dodd R J, Clark C W, Ruprecht P A and Burnett K 1996 *Phys. Rev. A* **53** R1950
- [15] Holland M J, Jin D S, Chiofalo M L and Cooper J 1997 *Phys. Rev. Lett.* **78** 3801
- [16] Proukakis N P, Burnett K and Stoof H T C 1998 *Phys. Rev. A* **57** 1230
- [17] Edwards M, Ruprecht P A, Burnett K, Dodd R J and Clark C W 1996 *Phys. Rev. Lett.* **77** 1671
- [18] Dodd R J, Edwards M, Clark C W and Burnett K 1998 *Phys. Rev. A* **57** R32
- [19] Taha T R and Ablowitz M J 1984 *J. Comp. Phys.* **55** 203
- [20] Javanainen J 1996 *Phys. Rev. A* **54** R3722
- [21] Jackson B, McCann J F and Adams C S 1998 *Phys. Rev. Lett.* **80** 3903
- [22] Ballagh R J, Burnett K and Scott T F 1997 *Phys. Rev. Lett.* **78** 1607
- [23] Steck H, Naraschewski M and Wallis H 1998 *Phys. Rev. Lett.* **80** 1
- [24] Zhang W and Walls D F 1998 *Phys. Rev. A* **57** 1248
- [25] Taubes G 1997 *Science* **275** 617
- [26] Nozières P and Pines D 1990 *The Theory of Quantum Liquids, Vol II* (Redmond City: Addison-Wesley)
- [27] Press W H, Flannery B P, Teukolsky S A and Vetterling W T 1989 *Numerical Recipes* (Cambridge: Cambridge University Press)
- [28] Feit M D, Fleck Jr J A and Steiger A 1982 *J. Comp. Phys.* **47** 412
- [29] Adams C S and Riis E 1997 *Prog. Quantum Elec.* **21** 1